Int.J.Curr.Res.Aca.Rev.2026; 14(11): 101-116

International Journal of Current Research and Academic Review

ISSN: 2347-3215 (Online) Volume 14 Number 11 (November-2026)

Journal homepage: http://www.ijcrar.com

doi: https://doi.org/10.20546/ijcrar.2026.1411.012

Reduced-Order Modelling of Concentrated-Leak Internal Erosion in the Former Zoungou Dam Embankment (Ganzourgou, Burkina Faso): Pipe Growth and Breach-Time Assessment

Mady Sawadogo[1*], Ulrich Landry Compaoré[2], Justin Tegawendé Zaïda[2] and David Yemboini Kader Toguyeni[2]

[1]*Université Joseph KI-ZERBO, Ouagadougou, Burkina Faso*
[2]*École Polytechnique de Ouagadougou, Ouagadougou, Burkina Faso*

**Corresponding author*

Abstract

Concentrated leak internal erosion is one of the main failure mechanisms affecting earth-fill dams. This study implements, in COMSOL Multiphysics, the reduced-order piping erosion model proposed by Bonelli *et al.,* (2007) and extended by Lachouette and Bonelli (2008), and applies it to the former breached embankment of the Zoungou Dam, located in Ganzourgou Province, Burkina Faso. The model is formulated as a system of three coupled global ordinary differential equations which describes the evolution of the erosion pipe radius R(t), the upstream reservoir level $H_{amont}(t)$, and the cumulative volume of eroded material $Vol_{érodé}(t)$. The embankment material was characterized by geotechnical identification tests, especially, sieving analysis, sedimentometry and Atterberg limits. Pending Hole Erosion Tests (HET),, the direct reference method for determining the critical erosion stress τ_c and the erosion coefficient K_{er}, these parameters were estimated from empirical correlations based on the plasticity index, fines content, and dry density of the material. The reference scenario, applied to the 6.5 m high structure with an initial defect of 10 cm in radius, results in a failure time of 5.24 hours for a total eroded volume of 994.47 m^3. The numerical solution is verified by comparison with an analytical solution based on a constant hydraulic load, with a discrepancy of less than 2.1%. A univariate sensitivity analysis of six parameters (τ_c, k_{er}, R_0, R_{max}, H_{aval} and λ_f) shows that the failure time is dominated by the erosion coefficient k_{er} and the hydraulic load, while the critical stress τ_c has only a negligible influence under these conditions.

Article Info

Received: 22 September 2026
Accepted: 31 October 2026
Available Online: 20 November 2026

Keywords

Earth dam, internal erosion, erosion model, COMSOL Multiphysics, embankment dam failure.

Introduction

Internal erosion is recognized as one of the main causes of failure of embankment dams and dikes, alongside overtopping. According to the ICOLD classification (2017), it encompasses several distinct mechanisms: concentrated leak erosion, backward erosion piping, suffusion and contact erosion. The present work deals specifically with concentrated leak erosion, which corresponds to the growth of a pre-existing defect under the effect of hydraulic friction.

This mechanism manifests itself through the formation and progressive enlargement of a pipe within the body of the structure or its foundation, under the effect of the seepage flow, until the embankment above the pipe collapses and a breach opens that may lead to the complete failure of the structure. Predicting the time

remaining between the detection of a defect and failure is therefore a major issue for risk management and emergency planning, particularly for the many small earth dams, often old and poorly instrumented.

Bonelli *et al.,* (2007) proposed a reduced-order model describing the evolution of a cylindrical erosion pipe, coupling a threshold erosion law with a simplified hydraulic balance of the flow in the pipe.

This model was subsequently extended by Lachouette *et al.,* (2008) and Bonelli *et al.,* (2008) to the scale of the structure, by coupling the evolution of the pipe with the progressive drawdown of the upstream reservoir and by proposing simplified expressions for the time remaining before failure.

The present work implements this reduced-order model in COMSOL Multiphysics and applies it to the former embankment of the Zoungou dam, located in Ganzourgou Province (Burkina Faso) at coordinates 12°7'30.46"N; 0°31'1.96"W, with the following objectives: (i) to characterize the embankment material from a geotechnical standpoint, (ii) to simulate the time evolution of the erosion pipe radius and of the volume of eroded material for a representative defect scenario, (iii) to identify the conditions leading to failure of the structure, and (iv) to quantify, through a sensitivity analysis, the relative influence of the geotechnical and hydraulic parameters of the problem on the predicted failure time.

Materials and Methods

Presentation of the site

The Zoungou dam is an earth embankment located in the south-east of Zoungou village, in Ganzourgou Province, Oubri region, Burkina Faso. It was built between 1991 and 1993 to improve the living conditions of local populations, through irrigation and livestock watering, like many small dams of the same type in the country.

The structure studied corresponds to the original embankment, which failed following a heavy rainfall in the night of 24 to 25 June 2021; the material characterized in this study comes from its fill body.

As a new embankment was subsequently built upstream, the structure analysed is referred to hereafter as the "former embankment". The erosion pipe is assumed to develop through the body of the embankment, at the base of the structure. The geometric parameters of the simulated scenario, in particular the height of the structure at the pipe location and the length of the pipe crossing the fill, are given in Table 3. The location of the study site is shown in Figure 1.

Figure.1 Location of the study site.

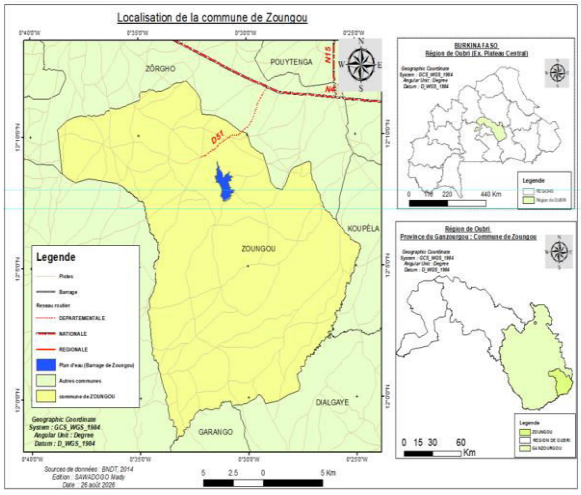

Figure.2 Illustration of an erosion pipe in an earth structure, according to Lachouette *et al.,* (2008).

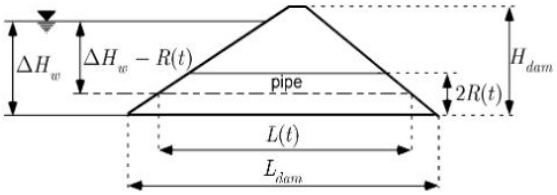

Geotechnical identification tests

The material forming the body of the embankment was characterized by a series of tests carried out in accordance with the standards in force, commonly applied in local geotechnical practice. These are:

- particle-size analysis by sieving (NF P 94-056);
- particle-size analysis by sedimentometry (NF P 94-057);
- determination of the Atterberg limits (NF P 94-051);
- determination of the density of solid particles (NF P 94-054);
- determination of the compaction references (Proctor test) (NF P 94-093).

The results obtained from these tests are presented in Figure 3 and in Table 1.

Table.1 Summary of the results of the geotechnical identification tests on the material of the former Zoungou embankment

Parameter	Value	Unit / Standard
Clay content (Ø ≤ 2 µm)	32.00	% / NF P 94-057
Silt content (2 µm < Ø ≤ 63 µm)	26.00	% / NF P 94-057
Sand content (63 µm < Ø ≤ 2 mm)	37.00	% / NF P 94-056
Gravel content (2 mm < Ø ≤ 20 mm)	5.00	% / NF P 94-056
Percentage passing the 80 µm sieve	74.03	% / NF P 94-056
Cobble content (Ø > 20 mm)	0.00	% / NF P 94-056
Diameter d50	0.03	mm
Liquid limit (L_L)	41	% / NF P 94-051
Plastic limit (L_P)	21.37	% / NF P 94-051
Plasticity index (I_P)	19.63	% / NF P 94-051
USCS classification	CL	-
LCPC classification	Ap	-
Density of solid particles (ρs)	2700	kg/m³ / NF P 94-054
Dry density at the Optimum Proctor	1785	kg/m³ / NF P 94-093

The particle-size distribution curve (Figure 3) and the plasticity index (I_P = 19.63%, L_L = 41%) place the material in the class of silty clays of moderate plasticity (CL according to the USCS classification and Ap according to the LCPC classification), with a predominant fine fraction (clay + silt) (58%) ahead of the sand fraction (37%) and a marginal coarse fraction (gravel) (5%). The percentage passing the 80 microns sieve is also noted: 74.03%. This composition, consistent with a compacted fill material typical of small earth dams, makes it a soil a priori susceptible to internal pipe erosion, which justifies the detailed characterization of its erodibility carried out in the following section. Indeed, this type of soil is well covered by the experimental devices used for the experimental characterization of internal erosion (Erosion Interne dans les Ouvrages Hydrauliques volume 1: méthodologie de caractérisation expérimentale, 2017).

Reduced-order model of pipe erosion

The reduced-order pipe erosion model is obtained from the conservation equations and the constitutive laws, by spatial integration over the cylinder representing the pipe (Bonelli and Brivois, 2008). It rests on three coupled physical components: a threshold erosion law at the soil-water interface, a solid mass balance describing the recession of the interface, and a quasi-steady hydraulic closure for the flow in the pipe.

Interface erosion law

The erosion of the material at the pipe wall is governed by a threshold law, classical in internal erosion, relating the density of eroded material flux per unit surface and time $\dot{m}$ to the difference between the hydraulic shear stress τ_b exerted by the flow on the wall and the critical erosion stress τ_c characteristic of the material:

$$\dot{m} = \begin{cases} k_{er}(\tau_b - \tau_c), & if\ \tau_b > \tau_c \\ 0 & , otherwise \end{cases} \quad (1)$$

With $\dot{m}$ the mass of eroded soil per unit surface and time (kg/m²/s), τ_b the shear stress of the fluid on the soil (Pa), τ_c the critical shear stress (Pa) and k_{er} the erosion coefficient (s/m).

Solid mass balance at the interface

The recession of the interface, i.e. the increase in the pipe radius R(t), results directly from the flux of eroded material through the solid mass balance:

$$\rho_d \frac{dR}{dt} = \dot{m} \quad (2)$$

where ρ_d is the dry density of the material (kg/m³).

Hydraulic closure and quasi-steady equilibrium

Assuming that the flow in the pipe is established over a time scale much shorter than that of pipe growth, Bonelli *et al.*, (2008) neglect the inertia terms in the momentum balance of the fluid. The balance between the driving pressure force and the wall friction force, over a pipe section of radius R and length L, leads to:

$$\tau_b = \frac{R\Delta P}{2L} = \frac{R\rho_f g \Delta H}{2L} \quad (3)$$

where $\Delta H = H_{amont} - H_{aval}$ is the driving hydraulic head (m), ρ_f the density of the fluid (water) (kg/m³), and **g** the acceleration of gravity (9.81 m/s²). This force-balance relation (3) is independent of the friction law adopted to close the system: it directly relates τb to the current

radius and to the driving head, whatever the hydraulic closure adopted.

To express the mean flow velocity **V**, a closure by a quadratic turbulent friction law is necessary. The present work adopts the Darcy-Weisbach convention, customary in pressurized-flow hydraulics:

$$h_t = \left(\frac{\lambda_f L}{D}\frac{V^2}{2g}\right) = \Delta H \quad (4)$$

Where: h_t is the hydraulic head (m); D: the pipe diameter (m) and L the pipe length (m). Combining equations (3) and (4) gives:

$$\tau_b = \left(\frac{1}{8}\right)\rho_f \lambda_f V^2 \quad (5)$$

with λ_f the Darcy-Weisbach friction coefficient. A constant value of $\lambda_f = 0.025$ is adopted in this work and corresponds to the usual order of magnitude for turbulent flow in a pipe of moderate to high roughness (Moody chart, 1944), consistent with the irregular wall of an erosion pipe formed in a mass of cohesive soil. It should be noted that Lachouette *et al.,* (2008) express this same friction law in the form τb = ρf fb V², with a coefficient fb directly defined as the ratio $\tau_b/(\rho_f V^2)$ and adopt a constant value of fb = 0.006. The equality of expressions (3) and (5) makes it possible to express the flow velocity explicitly as a function of the current radius and of the driving head:

$$V = \left(\frac{4g\Delta HR}{\lambda_f L}\right)^{1/2} \quad (5)$$

Hydraulic balance of the upstream reservoir and eroded volume

At the scale of the structure, the leakage discharge $Q = \pi R^2 V$ progressively lowers the level of the upstream reservoir, whose evolution is described by the balance:

$$\frac{dH_{amont}}{dt} = \frac{Q_{in} - Q_{out}}{S_{res}(H_{amont})} \quad (6)$$

where $S_{res}(H_{amont})$ is the free surface area of the upstream water body at elevation H_{amont}, given by the height–area curve of the reservoir, and Qin the possible inflow, taken as zero in this study. The cumulative volume of eroded material is obtained by time integration of the erosion flux over the lateral surface of the pipe:

$$\frac{dVol_{érodé}}{dt} = \frac{2\pi R\, L\dot{m}}{\rho_d} \quad (7)$$

Failure criterion

The reduced-order model explicitly describes only the growth phase of the pipe in closed cylindrical form. Beyond a critical radius R_{max}, the thickness of soil remaining above the pipe (the "roof") can no longer carry its own weight by arching effect and collapses, paving the way for the rapid widening of a breach. The failure time $t_{rupture}$ is thus defined, in this work, as the instant when R(t) reaches R_{max}. In the absence of a stability calculation specific to the structure studied, the critical radius was taken equal to $R_{max} = H/2$ (H being the height of the embankment at the pipe location), in accordance with the study of the orders of magnitude of the maximum pipe diameter before roof collapse reported by Bonelli and Benahmed (2010) on the basis of a compilation of real cases of failure by piping.

Identification of the erodibility parameters

Pending Hole Erosion Tests (HET), which would allow a direct determination of τc and ker, these two parameters were estimated by means of empirical correlations relating the erodibility of the soil to its usual geotechnical characteristics (plasticity index, fines content, dry density). The critical stress was thus estimated from the correlation of Smerdon and Beasley (1961) based on the plasticity index (8).

The erosion index Ie was estimated from the empirical correlation proposed by Temple and Hanson (1994) (9), as reported by Lachouette and Bonelli (2008).

This index is then related to the erosion coefficient through relation (10), in accordance with the definition used in the methodology of Wan and Fell (2004)

$$\tau_c = 0.16 I_P{}^{0.84} \quad (8)$$

$$I_e = 2 + 0.052(\rho_d/\rho_f)^{3.1} C^{0.406} \quad (9)$$

$$I_e = -log_{10}(K_{er}) \quad (10)$$

Which gives $K_{er} = 10^{-Ie}$

where I_P is the plasticity index (%), C the clay fraction of the material, i.e. the content of particles smaller than 2 µm (%), ρd the dry density of the soil (kg/m³) and ρ_f the density of water (kg/m³). Ie is the erosion index (Wan & Fell scale), and k_{er} the erosion coefficient (s.m^{-1}).

The values obtained from these equations are listed in Table 2.

Table.2 Erodibility parameters derived from the empirical correlations

Quantity	Symbol	Value	Unit
Erosion index	Ie	3.28	-
Critical erosion stress	τ_c	1.951	Pa
Erosion coefficient	k_{er}	5.249×10^{-4}	s/m

Numerical implementation

The system of equations (1)-(7) was implemented in COMSOL Multiphysics 6.2 using the Global ODEs and DAEs interface (Ordinary Differential Equations) and (Differential-Algebraic Equations), in the form of a system of three coupled ordinary differential equations for the state variables R(t), $H_{amont}(t)$ and $Vol_{érodé}(t)$, solved by an implicit time-stepping scheme (BDF) with adaptive step size.

The threshold erosion law (Eq. 1), whose derivative is discontinuous, was regularized by a cubic smoothing function (COMSOL flc2hs function) over a width equal to 5% of τ_c, in order to ensure convergence of the nonlinear solver without significantly altering the physical behaviour of the threshold. A maximum time step of 10 s was imposed in the vicinity of failure in order to correctly resolve the quasi-exponential acceleration phase of pipe growth. The computation was stopped at the failure time (where $R = R_{max}$) by a solver stop condition, triggered at the first crossing of the threshold, with the failure time estimated by linear interpolation between the last two times steps bracketing the crossing. The upstream water-body surface area $S_{res}(H_{amont})$ was specified by an interpolation function built from the measured height-area (bathymetric) curve of the reservoir (*Rapport d'études de reconstruction du Barrage de Zoungou dans la province du Ganzourgou, région du Plateau Central, GROUPEMENT AC3E / GERTEC Ingénieurs Conseils, 2023)*, covering the range 0-7 m.

Results and Discussion

Analytical solution

An analytical solution can be established under the assumption of a driving head ΔH frozen at its initial value $\Delta H_0 = H_{amont,0} - H_{aval}$. In this case, combining equations (3) and (5), the wall stress becomes directly proportional to the radius,

$$\tau_b = aR \text{ with: } a = \frac{\rho_f g \Delta H_0}{2L} \quad (11)$$

The solid mass balance (Eq. 2) then reduces to a first-order linear differential equation in R, with solution:

$$R(t) = (R_0 - R_c)e^{\alpha t} + R_c \quad (12)$$

with $\alpha = k_{er}a/\rho_d$ and R_c the equilibrium radius (where $\tau b = \tau c$): $R_c = 2L\tau_c/(\rho_f g \Delta H_0)$ (13)

hence an approximate analytical failure time, valid for $R_0 \gg R_c$:

$$t_{rupture,analytique} \approx \left(\frac{1}{\alpha}\right)\ln\left(\frac{R_{max}}{R_0}\right) \quad (14)$$

Table.4 Comparison of the numerical and analytical solutions

Quantity	Value
Initial driving head ΔH_0	3.95 m
Equilibrium radius R_c	≈ 3 mm
Growth rate α	1.89×10^{-4} s^{-1}
Analytical failure time	5.135 h (18.486 s)
Numerical failure time	5.244 h (18.878 s)
Relative difference	≈ 2.1%

The 2.1% difference between the two approaches is consistent with the expected physical behaviour: the progressive drop of the upstream level in the numerical calculation (not accounted for by the frozen-head assumption of the analytical solution) slightly reduces the driving head over time, which very slightly slows the growth of the pipe and lengthens the numerical failure time relative to the analytical time. This agreement, obtained on a parameter independent of the model calibration, provides a partial verification of the numerical implementation under the stated simplifying assumptions; however, it does not by itself constitute a physical validation of the actual failure of the structure.

Reference solution

The results obtained from the modelling with the reference parameter values are presented as follows.

First, Figure 4 shows the time evolution of the pipe radius R(t) obtained numerically, compared with the

closed-form analytical solution established, for a constant driving head, in the section devoted to the analytical verification. The growth of R is initially slow, then accelerates quasi-exponentially as failure approaches. This dynamic reflects the positive feedback of the model: the increase in radius raises the flow velocity, then the wall stress and the erosion flux, which further accelerates the growth of the pipe.

Figure.4 Time evolution of the erosion pipe radius R(t): comparison between the COMSOL numerical solution and the analytical solution at constant hydraulic head.

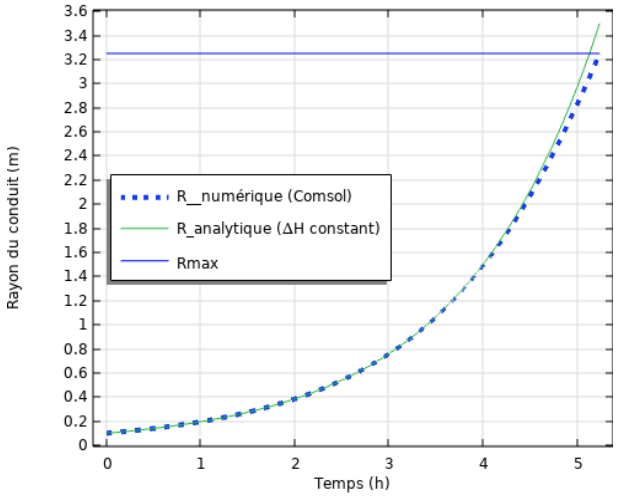

Next, Figure 5 shows the evolution of the leakage discharge $Q(t) = \pi R^2 V$, which naturally follows the same accelerating dynamic as R(t).

Figure.5 Time evolution of the leakage discharge Q(t).

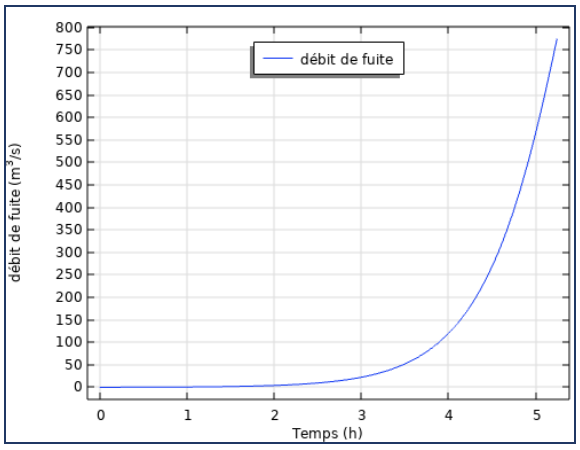

The cumulative volume of eroded material $Vol_{érodé}(t)$, shown in Figure 6, increases monotonically and follows the same acceleration signature at the end of the simulation.

Figure.6 Cumulative volume of eroded material $Vol_{érodé}(t)$.

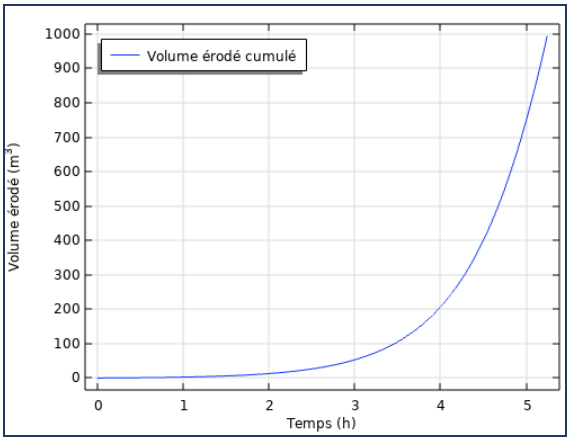

The evolution of the reservoir level $H_{amont}(t)$, shown in Figure 7, indicates a limited drawdown (0.75 m) over the total duration of the phenomenon; the drop in level becomes significant only in the last instants before failure.

Figure.7 Evolution of the upstream reservoir level $H_{amont}(t)$, compared with the downstream level Haval (constant).

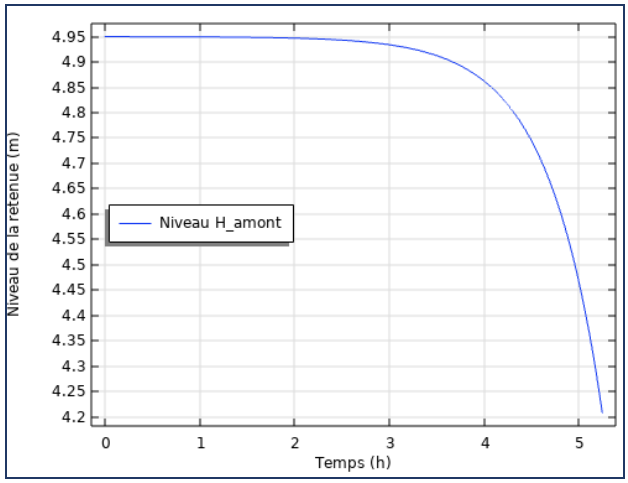

Finally, Figure 8 compares the wall friction stress $\tau_b(t)$ with the critical stress τ_c. Since the initial radius R_0 = 0.10 m is much larger than the equilibrium radius Rc ≈ 3 mm (the radius for which $\tau_b = \tau c$), the wall stress is already far above the critical threshold from the initial instant: erosion therefore starts immediately, and the

limiting factor of the process is the growth kinetics rather than the initiation itself.

Figure.8 Comparison between the wall friction stress $\tau_b(t)$ and the critical erosion stress τ_c (logarithmic scale).

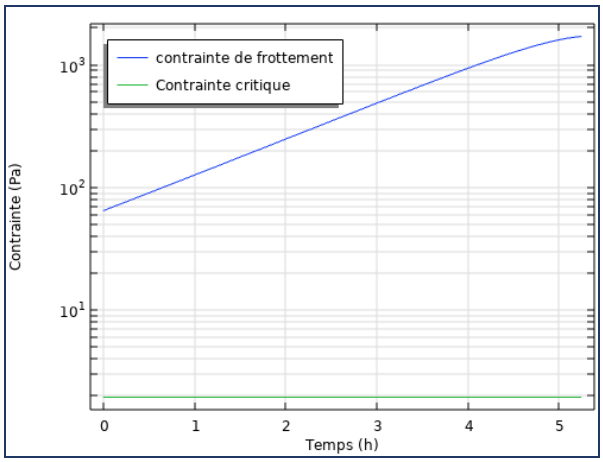

The final leakage discharge (774.2 m³/s) should be interpreted as a limiting value computed at the instant R_{max} is reached. At this stage, the closed cylindrical pipe presumably ceases to be a physical representation, so that this value should not be equated with the actual breach hydrograph.

Table.5 Results of the reference scenario at the failure time

Quantity	Value	Unit
Time to failure	5.24	h
Final pipe radius	3.249 (≈ R_{max})	m
Final upstream level	4.21	m
Final driving head ΔH	3.21	m
Total eroded volume	994.47	m³
Final leakage discharge	774.2	m³/s

A simple geometric consistency check applied to the final radius ($\pi L(R_{max}^2 - R0^2) \approx 994.94$ m³) gives a result very close to the calculated cumulative eroded volume (994.47 m³), which is physically expected.

Sensitivity analysis

A univariate sensitivity analysis was carried out on six parameters of the model: the critical erosion stress $\boldsymbol{\tau_c}$, the erosion coefficient $\mathbf{k_{er}}$, the initial defect radius $\mathbf{R_0}$, the critical failure radius $\mathbf{R_{max}}$, the downstream water level $\mathbf{H_{aval}}$ (which controls, together with the upstream level, the driving head ΔH_0) and the Darcy-Weisbach friction coefficient $\boldsymbol{\lambda_f}$.

For each parameter, the other quantities of the model are kept at their reference value.

Sensitivity to the critical stress τ_c

The critical stress τ_c was tested between 1 and 3 Pa (factor 3), around the reference value of 1.95 Pa.

Figure.9 Sensitivity of the failure time to the critical erosion stress τ_c.

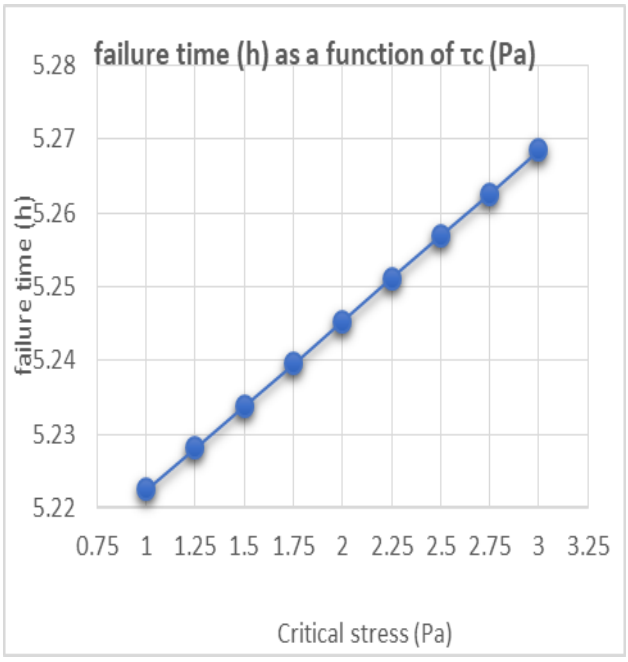

Over the entire range tested, the failure time varies by less than 1% (factor 1.009), a quasi-negligible influence.

This result, a priori counter-intuitive for a threshold parameter, is directly explained by the analytical solution (Eqs. 13 and 14):

$\boldsymbol{\tau_c}$ does not enter the growth rate $\boldsymbol{\alpha}$, but only the equilibrium radius $\mathbf{R_c}$, which remains of the order of a millimetre over the whole range tested, and therefore much smaller than the initial radius $\mathbf{R_0}$ = 0.10 m.

Sensitivity to the erosion coefficient ker

The coefficient k_{er} was tested over nearly two orders of magnitude, from 2×10^{-4} to 5×10^{-3} s/m.

Figure.10 Sensitivity of the failure time to the erosion coefficient k_{er} (log-log scale).

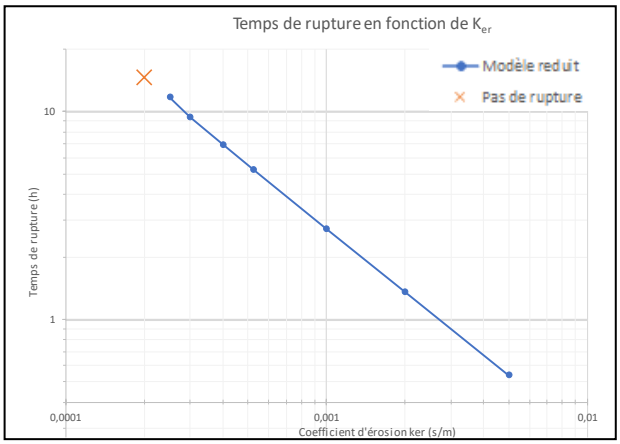

For $k_{er} \geq 2.5\times10^{-4}$ s/m, failure goes on and the failure time varies from 11.7 h to 0.54 h, i.e. a factor of 21.7 for a factor of 20 on k_{er}, which confirms the expected power law $t_{rupture} \propto 1/ker$ (Eqs. 13 and 14). However, for $k_{er} = 2\times10^{-4}$ s/m, no failure occurs; the upstream level reaches the downstream level (14.7 h) while the pipe radius has reached only 2.99 m, i.e. 92% of R_{max}. A critical threshold of k_{er} would therefore lie between 2.0 and 2.5×10^{-4} s/m, i.e. a factor of 2 to 2.5 below the reference value of 5.0249×10^{-4} s/m. This parameter appears to be the most decisive one in the model.

Sensitivity to the initial radius R0

The initial radius was tested between 0.02 and 0.30 m.

Figure.11 Sensitivity of the failure time to the initial defect radius R_0 (semi-logarithmic scale).

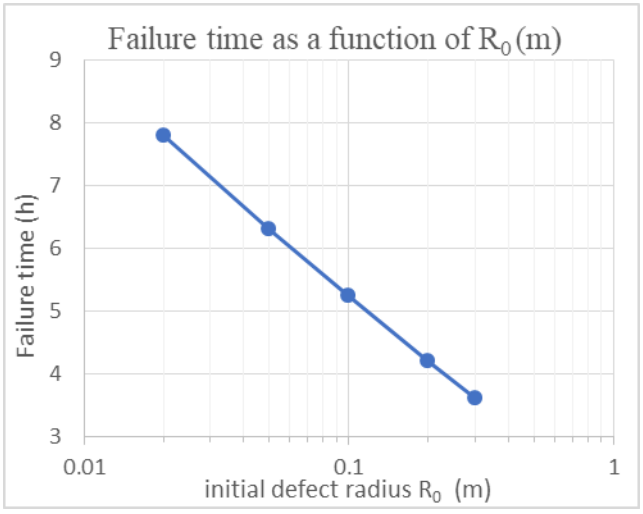

The expected logarithmic dependence (Eq. 14) results in a moderate sensitivity: for a factor 15 variation of R_0, the failure time varies by only a factor of 2.16.

Sensitivity to the critical radius Rmax

R_{max} was tested between 0.3 and 0.7 times the height of the structure, bracketing the reference estimate (0.5×H), and covering the range of orders of magnitude reported by Bonelli and Benahmed (2010).

Figure.12 Sensitivity of the failure time to the critical roof-collapse radius R_{max}.

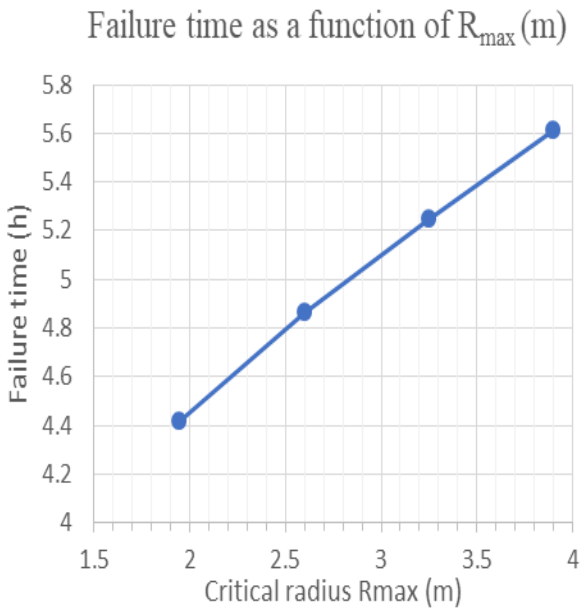

The effect of Rmax is the smallest of all the non-negligible parameters tested; for a factor 2.0 variation, the failure time varies by only a factor of 1.27.

This result indicates limited sensitivity to Rmax over the tested range; however, it does not independently validate the assumed roof-collapse criterion Rmax = H/2.

On the other hand, for Rmax=4.55 m there is no failure. The pipe stops at a radius of about 4.39 m (0.68×H, i.e. 96.6% of Rmax) when the reservoir has been drawn down to the downstream level.

Sensitivity to the downstream level Haval

The downstream level was tested between 0 and 2 m, bracketing the reference value of 1 m.

Figure.3 Particle-size distribution curve of the Zoungou embankment material (former embankment)

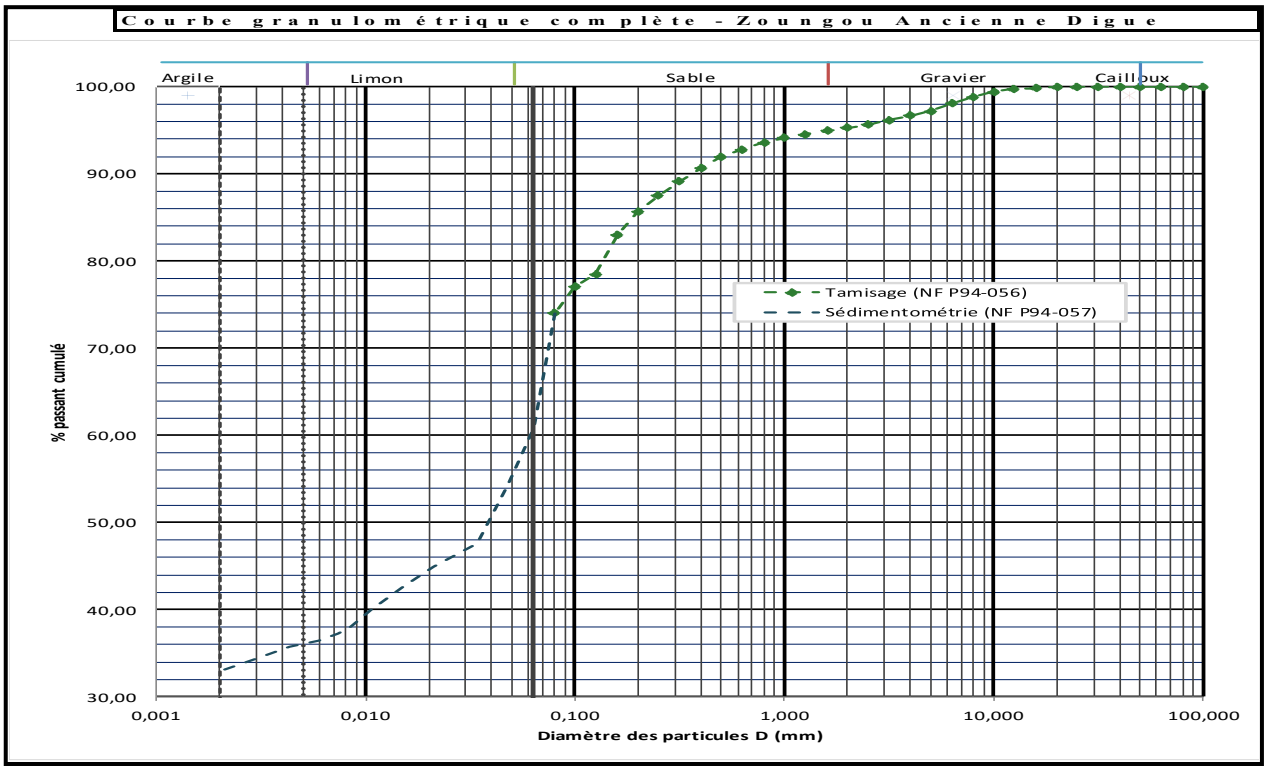

Figure.15 Evolution of the pipe radius R(t) and of the reservoir level $H_{amont}(t)$.

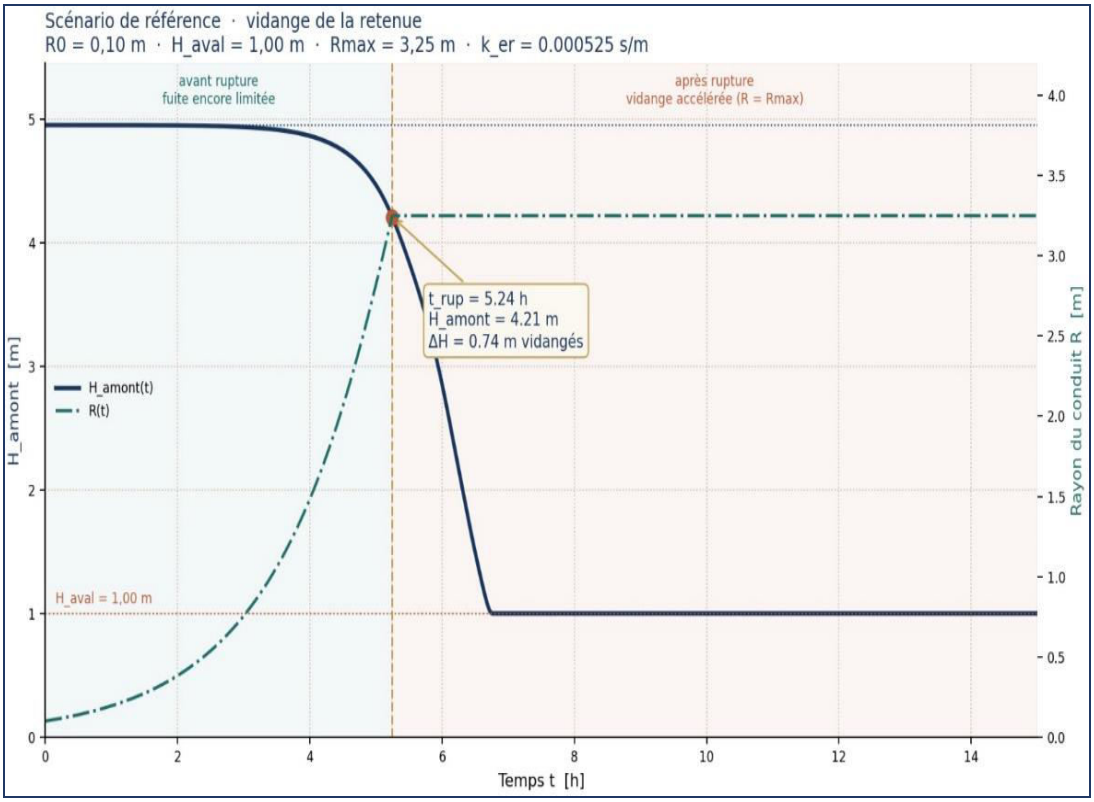

Figure.16 Evolution of the leakage discharge $Q_{débit}(t)$

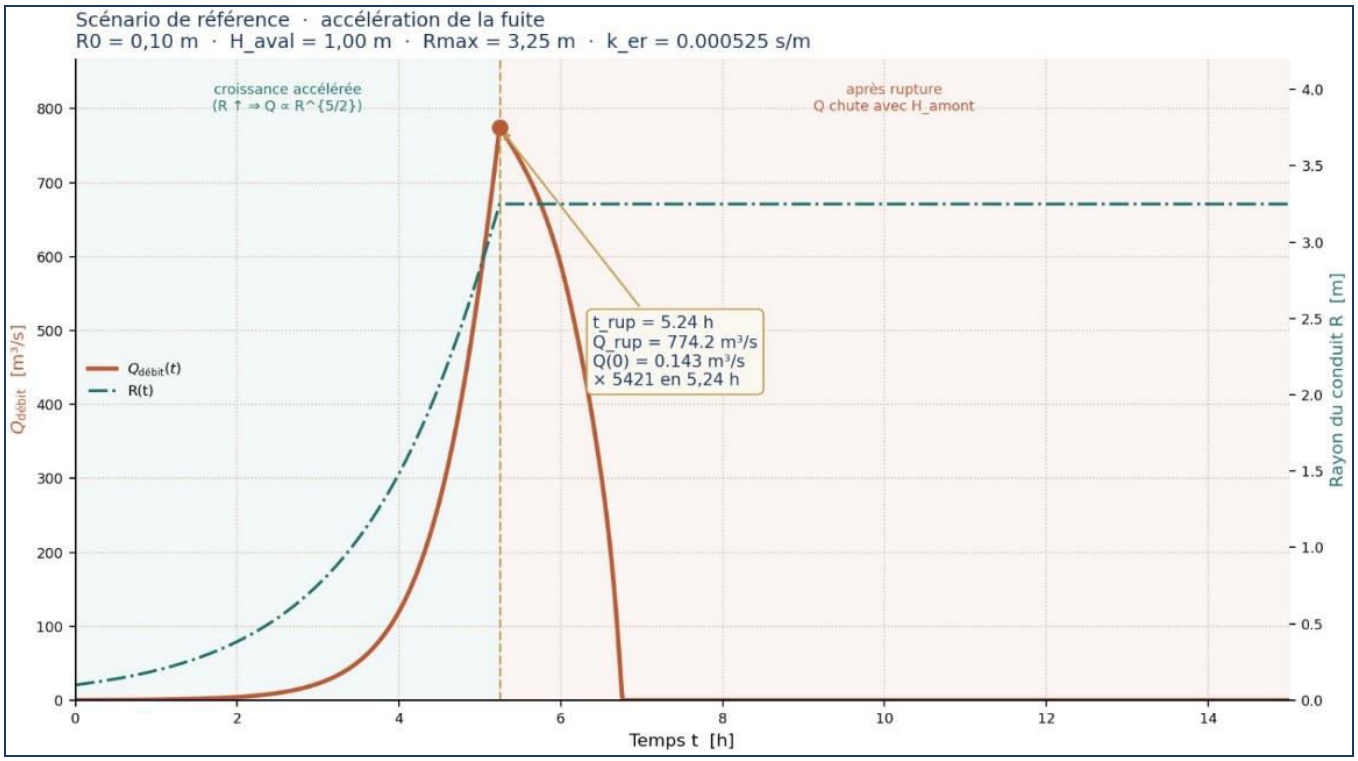

Figure.17 Sensitivity on the evolution of the reservoir level $H_{amont}(t)$

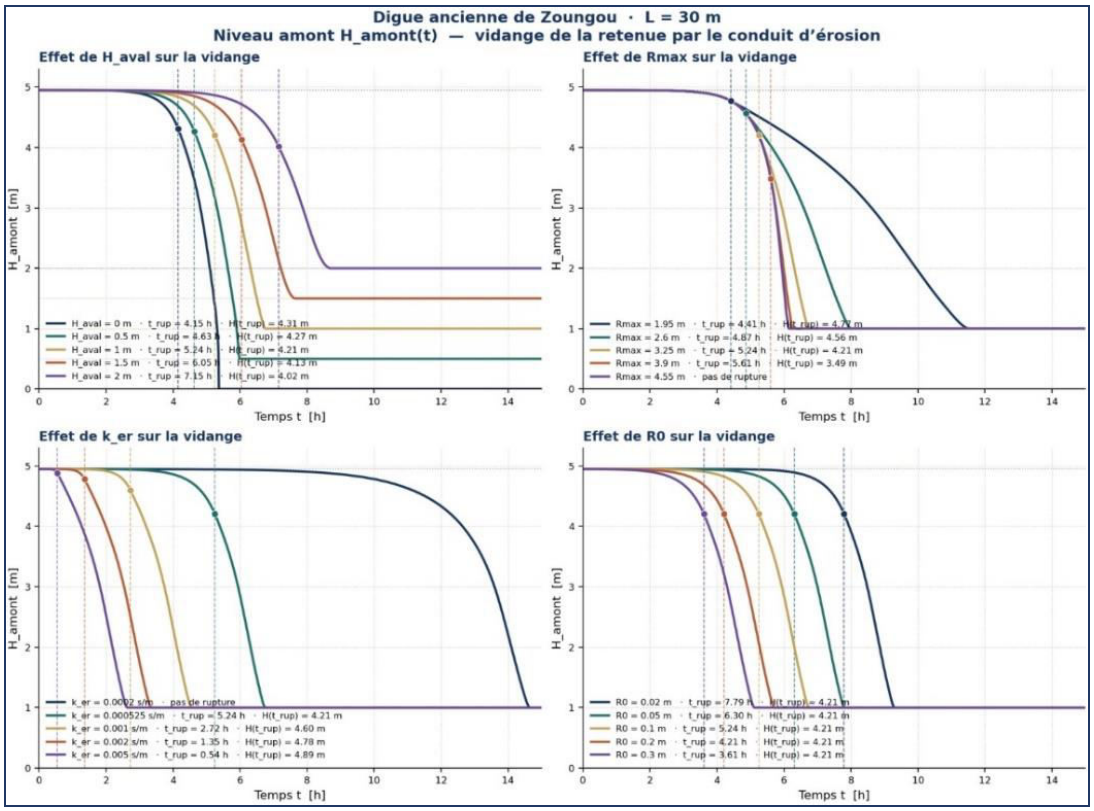

Figure.18 Sensitivity on the evolution of the pipe radius R(t)

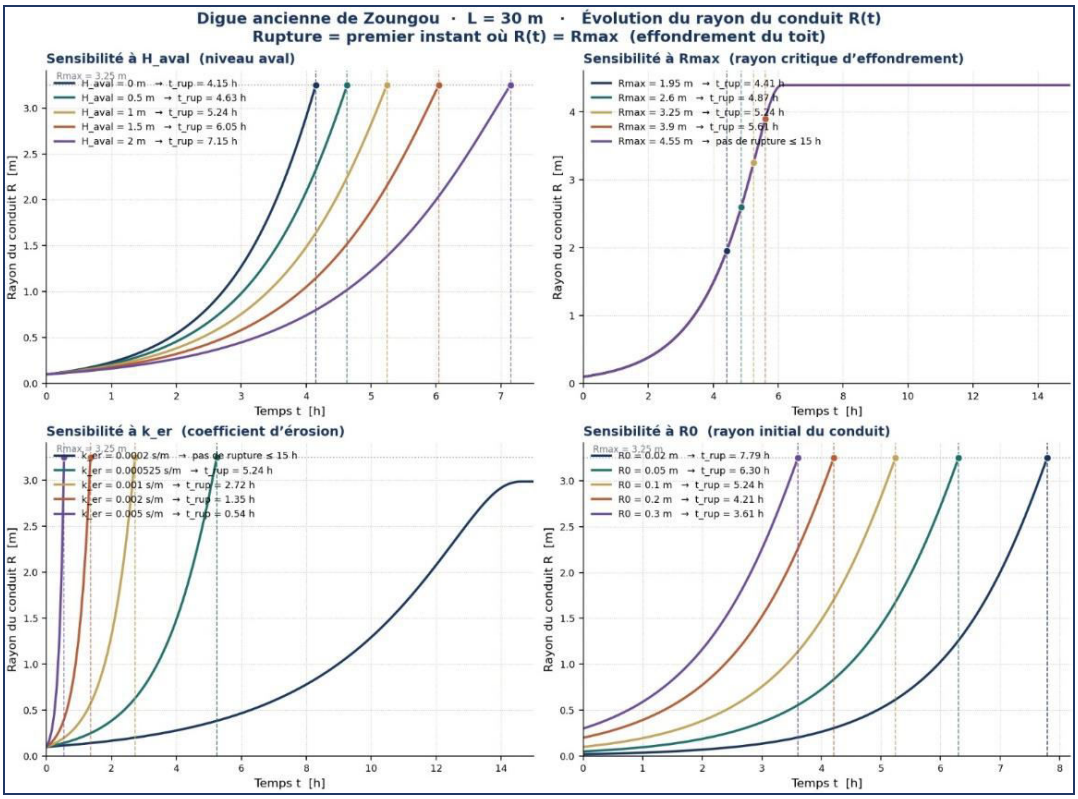

Figure.19 Sensitivity on the evolution of the discharge $Q_{débit}$

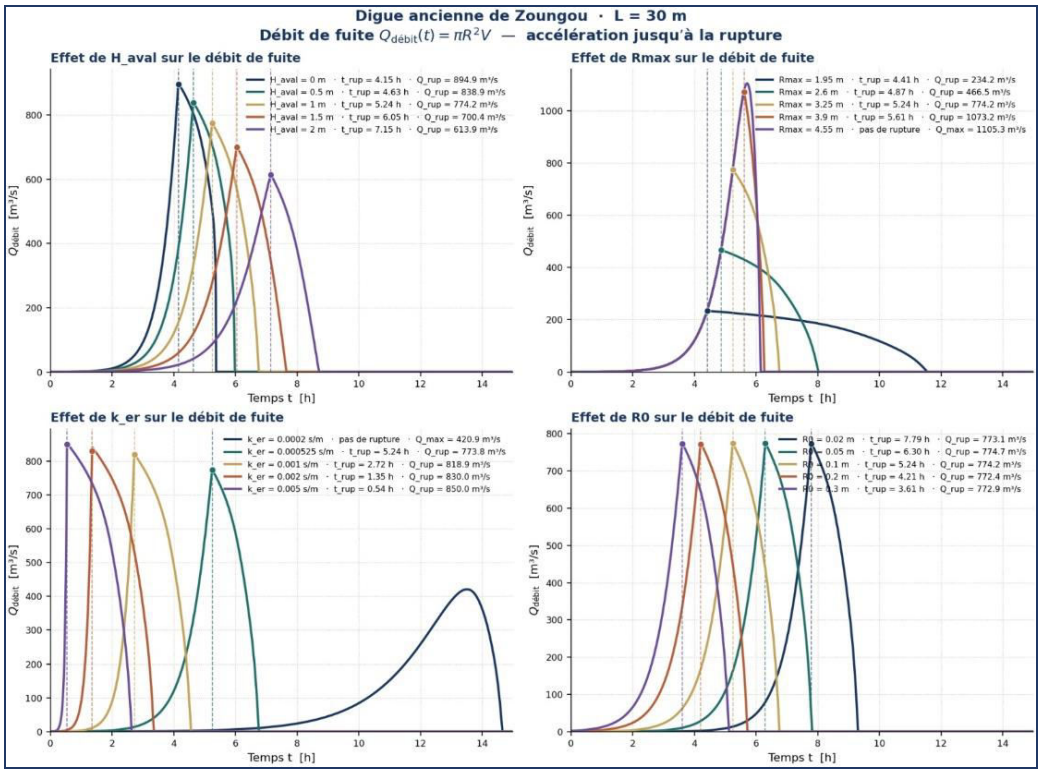

Table.3 Geometric and hydraulic parameters of the reference scenario

Quantity	Symbol	Value	Unit	Origin
Pipe length	L	30	m	Values given by the geometry of the embankment
Height of the structure at the pipe location	H	6.5	m	Values given by the geometry of the embankment
Initial defect radius	R_0	0.1	m	Value adopted as the initial defect scenario
Critical roof-collapse radius	R_{max}	3.25 (≈ H/2)	m	Simplified assumption inspired by the orders of magnitude reported by Bonelli and Benahmed
Initial upstream reservoir level	$H_{amont},0$	4.95	m	Highest Water Level (HWL) of the water body
Downstream level	H_{aval}	1	m	based on the spillway stability calculation assumptions
Friction coefficient (Darcy-Weisbach)	λ_f	0.025	-	-

Table.6 Summary of the univariate sensitivity analysis

Parameters	Range tested (factor)	Effect on $t_{rupture}$ (factor)	Nature of the dependence
k_{er}	x20	x21.7	Strong
R_0	x15	x2.16	Moderate
H_{aval} (via ΔH_0)	x1.68 on ΔH_0	x1.72	Moderate
R_{max}	x2.0	x1.27	Weak
λ_f	x3.33	x1.015	Negligible
τ_c	x3	x1.009	Negligible

Figure.13 Sensitivity of the failure time to the downstream water level H_{aval}.

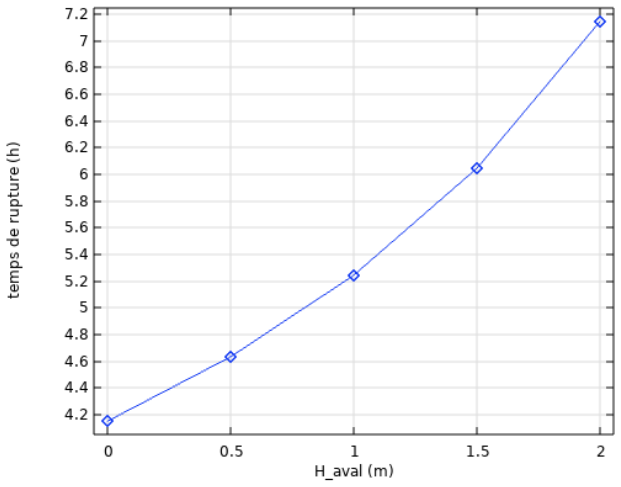

The sensitivity is strong and quasi-linear: over this range, the failure time varies by a factor of 1.72, in proportion to the inverse of the driving head ΔH_0, in accordance with Equation (13).

Sensitivity to the friction coefficient

The Darcy-Weisbach friction coefficient λ_f, whose value is not directly given by the Moody chart for this type of pipe, was tested between 0.015 and 0.05, i.e. a fairly wide range (factor 3.3) largely bracketing the usual values for rough pipes.

Figure.14 Sensitivity of the failure time to the friction coefficient λf.

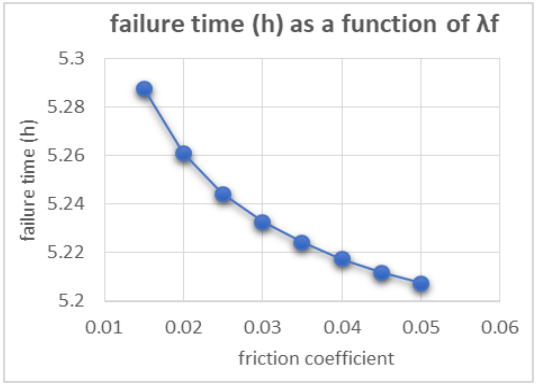

Unlike the other parameters, λ_f does not enter directly into the equations related to the solid mass results. The wall stress τb is fixed by the force balance (Eq. 3), independently of the hydraulic closure. λ_f acts only on the flow velocity V (Eq. 5), and hence on the leakage discharge Q and on the drawdown rate of the upstream reservoir (Eq. 6). Its influence on the failure time is therefore indirect and manifests itself through a feedback loop; a higher value of λf reduces V for a given radius and driving head, which reduces Q and slows down the drawdown of the reservoir, and the driving head ΔH(t) then remains close to its initial value for longer, which slightly accelerates erosion (τb being proportional to ΔH) and shortens the failure time. This mechanism is confirmed numerically; over the range tested, the failure time varies by a factor of only 1.015, hence a negligible sensitivity to λ_f.

Time evolution of the reference scenario

The reduced-order model presented above stops, by construction, at the failure time ($R = R_{max}$), beyond which the growth of the pipe in closed cylindrical form is no longer representative. In order to illustrate qualitatively the behaviour of the system beyond this instant, the reference scenario was extended by fixing the pipe radius at its critical value ($R = R_{max}$, the roof having collapsed but the subsequent widening of the breach not being modelled) and by continuing the integration of the hydraulic balance of the upstream reservoir (Eq. 6) and of the associated leakage discharge through this now-fixed opening.

The results are shown in the curves of Figures 15 and 16 that follow. Figure 15 jointly shows the evolution of the pipe radius R(t) and of the reservoir level $H_{amont}(t)$ over the whole of this extended episode. Beyond $t_{rupture}$, with R now fixed at R_{max}, the upstream level continues to fall, even faster, until it reaches the downstream level ($H_{amont} \rightarrow H_{aval} = 1.00$ m) in a little less than one and a half additional hours, reflecting the almost complete emptying of the reservoir through the opening of maximum size.

Figure 16 shows, over the same period, the evolution of the leakage discharge $Q_{débit}(t) = \pi R^2 V$. It comes out that, the discharge increases rapidly as failure approaches. Moreover, immediately after failure, this discharge is briefly maintained (the radius remains stable, but the driving head is still substantial), before decreasing rapidly as the reservoir dries up, falling to zero when H_{amont} reaches H_{aval}.

Cross-confirmation of the asymptotic behaviour

Figures 17 to 19 revisit the sensitivity analysis (parameters H_{aval}, R_{max}, k_{er} and R_0) by presenting, for each parameter, the complete evolution of $H_{amont}(t)$ rather than only the failure time. They provide a twofold confirmation with respect to the results presented previously.

First, the qualitative sensitivity trends are fully confirmed: the failure time increases with H_{aval} (from 4.15 h to 7.15 h over the range tested) and decreases with R_0, in accordance with the sensitivity factors reported in Table 6.

Second, a self-arrest behaviour is noted for $R_{max} = 4.55$ m (Fig. 17): the upstream level dries up completely down to H_{aval} before the pipe reaches this critical radius. A similar behaviour is observed for a sufficiently low erosion coefficient ($k_{er} \lesssim 2\times10^{-4}$ s/m), the reservoir drying up before the erosion, too slow, could bring the pipe to $R_{max} = 3.25$ m.

The tornado diagram (Fig. 19) provides a visual summary of this hierarchy: the erosion coefficient k_{er} overwhelmingly dominates all the sources of uncertainty considered, followed by the initial radius R_0 and then the downstream level H_{aval}, while R_{max}, λ_f and τ_c exert only a secondary to negligible influence.

These results agree with the work of Bonelli *et al.*, (2008), which shows that the parameter k_{er} governs the rate of degradation by erosion and makes it possible to quantify the failure time of the structure.

Figure.20 Tornado diagram: range of the failure time obtained for each parameter over its tested range of variation, the vertical line indicating the reference scenario (5.24 h).

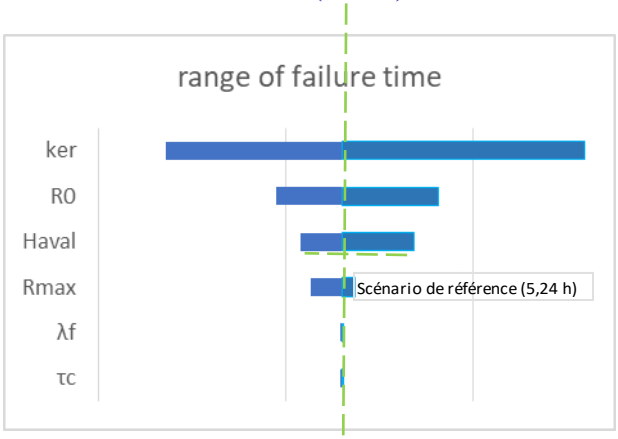

Ranking of the parameters and practical implications

The most significant result of this study is the demonstration of a very clear hierarchy among the parameters of the model; k_{er} overwhelmingly dominates the variability of the failure time, followed by the initial defect radius R_0 and the driving hydraulic head (via H_{aval}), whereas τc and λ_f, in the regime considered (initial defect much larger than the equilibrium radius), have only a negligible influence. An increase of k_{er} from 5.25×10^{-4} to 5×10^{-3} s/m reduces the failure time from 5.24 h to 0.54 h, whereas an increase of H_{aval} from 0 to 2 m delays failure from 4.15 to 7.15 h, owing to the reduction in the driving hydraulic head.

The weak influence of τ_c on the failure time, a priori counter-intuitive for a threshold parameter, is directly explained by the analytical solution (Eqs. 13 and 14); τ_c does not enter the growth rate α, but only the equilibrium radius Rc, which remains of the order of a millimetre over the whole range tested, and therefore much smaller than the initial radius R_0 = 0.10 m.

An operational recommendation follows for the Zoungou embankment and similar structures; in future campaigns to characterize internal erosion, additional efforts should be directed primarily towards the precise determination of k_{er}, for example by means of an HET test on the material, rather than towards the sole estimation of τc.

This hierarchy must nevertheless be read in light of the uncertainty on k_{er}, estimated here by empirical correlation. A direct measurement by HET test would therefore be the experimental priority to consolidate the quantitative scope of the results.

The existence of a self-arrest behaviour for R_{max} = 4.55 m and for sufficiently low values of the erosion coefficient ($k_{er} \lesssim 2\times10^{-4}$ s/m) (Fig. 10) is explained, respectively, by the fact that the upstream level dries up completely down to H_{aval} before the pipe reaches this critical radius, and by the fact that the reservoir dries up before the erosion, too slow, could bring the pipe to R_{max} = 3.25 m.

The quasi-exponential rise of the leakage discharge as failure approaches, followed by a rapid decrease once the breach geometry has stabilized, illustrated in Figure 15, illustrates a hypothetical post-threshold discharge trajectory under a fixed-opening assumption. It should not be interpreted as a validated breach hydrograph or used directly for downstream flood prediction without additional breach modelling and validation. By fixing R at Rmax after failure, the model does not represent the subsequent widening of the breach. This extension must therefore be read as a lower bound of the actual drawdown kinetics, and not as a quantitative prediction of the complete breach hydrograph.

Limitations of the reduced-order model

The reduced-order model rests on several simplifying assumptions whose limits must be made explicit. The quasi-steady flow assumption presupposes a separation of time scales between the establishment of the flow and the growth of the pipe; it remains consistent over most of the simulation, but its validity becomes more questionable in the very last instants before failure. The extreme leakage discharge obtained as R_{max} is approached indicates that the pipe then ceases to be a localized perturbation of the soil mass, which marks the limit of applicability of the reduced-order model. The critical radius R_{max}, estimated by a pragmatic approach consistent with Bonelli and Benahmed (2010), introduces an uncertainty that nevertheless appears limited according to the sensitivity analysis. Finally, since the erodibility parameters derive from empirical correlations rather than from a direct HET test, their own uncertainty, not quantified here, deserves to be explored by a probabilistic approach.

Perspectives

Several extensions of this work are envisaged. Carrying out an HET test on the Zoungou embankment material would make it possible to compare the measured erodibility parameters directly with the values derived from the empirical correlations used in this study.

A complementary 2D axisymmetric model, resolving the actual turbulent flow in the pipe coupled with a moving mesh representing the geometric evolution of the pipe, would make it possible to dispense with the empirical hydraulic closure (Eq. 4) and to assess its validity.

Finally, coupling the present model with a post-collapse breach model would make it possible to extend the prediction beyond the failure time, up to the estimation of the complete breach hydrograph, relevant for downstream flooding studies and for planning measures to protect the populations living near the dam.
In conclusion, this work presented the implementation, in COMSOL Multiphysics 6.2, of the reduced-order pipe

erosion model of Bonelli *et al.,* (2007) and of Lachouette and Bonelli (2008), applied to the former Zoungou embankment (Ganzourgou, Burkina Faso). The fill material was characterized by a series of standardized geotechnical tests, including particle-size analysis, Atterberg limits and the Proctor test. Pending HET tests, the erodibility parameters were estimated by empirical correlations. The reference scenario simulates the attainment of the failure criterion in 5.24 hours for an eroded volume of about 995 m³; this result is verified by comparison with a closed-form analytical solution with a difference of less than 2.1%, but must be regarded as a scenario-based estimate given the absence of direct experimental calibration of ker. The univariate sensitivity analysis on six parameters reveals a clear hierarchy, dominated by the erosion coefficient k_{er} and the driving hydraulic head, the critical stress τ_c having only a negligible influence in the regime studied. These results provide a useful basis for assessing the risk of failure by internal erosion of the Zoungou dam embankment and a first methodological milestone before extending the work to a 2D axisymmetric model of turbulent flow.

Acknowledgement

We would like to express our sincere gratitude to the African Water and Sanitation Association (AAEA) as part of its capacity-building programme for African actors in the water, sanitation and hygiene sector (Africap) for its financial contribution to the successful completion of our work.

References

AFNOR (1991) *NF P94-054. Sols: reconnaissance et essais. Détermination de la masse volumique des particules solides des sols. Méthode du pycnomètre à eau*. Paris: Association Française de Normalisation.

AFNOR (1992) *NF P94-057. Sols: reconnaissance et essais. Analyse granulométrique des sols. Méthode par sédimentométrie*. Paris: Association Française de Normalisation.

AFNOR (1993) *NF P94-051. Sols: reconnaissance et essais. Détermination des limites d'Atterberg. Limite de liquidité à la coupelle. Limite de plasticité au rouleau*. Paris: Association Française de Normalisation.

AFNOR (1996) *NF P94-056. Sols: reconnaissance et essais. Analyse granulométrique. Méthode par tamisage à sec après lavage*. Paris: Association Française de Normalisation.

AFNOR (2014) *NF P94-093. Sols: reconnaissance et essais. Détermination des références de compactage d'un matériau. Essai Proctor normal. Essai Proctor modifié*. Paris: Association Française de Normalisation.

Bonelli, S. and Benahmed, N. (2010) 'Piping flow erosion in water retaining structures: inferring erosion rates from hole erosion tests and quantifying the failure time', in *IECS 2010, 8th ICOLD European Club Symposium. Dam Safety: Sustainability in a Changing Environment*. Innsbruck, Austria, September 2010.

Bonelli, S., Benahmed, N., Philippe, P., Bernard, A., Gremeaux, Y. and Nunes, G. (2008) 'Évaluer le temps de rupture d'une digue en remblai érodée par conduit traversant', *Sciences Eaux & Territoires*, (Spécial Ingénieries-EAT-26), pp. 85–94.

Bonelli, S., Brivois, O. and Benahmed, N. (2007) 'Modélisation du renard hydraulique et interprétation de l'essai d'érosion de trou', *Revue Française de Géotechnique*, 118, pp. 13–22. https://doi.org/10.1051/geotech/2007118013

Bridle, R. (2017) 'Internal erosion mechanics and risk estimation based on ICOLD Bulletin 164', in *Geo-Risk 2017*. Denver, Colorado, June 2017. Reston, VA: American Society of Civil Engineers. https://doi.org/10.1061/9780784480724.013.

Brown, G.O. (2003) 'The history of the Darcy-Weisbach equation for pipe flow resistance', in Rogers, J.R. and Fredrich, A.J. (eds) *Environmental and Water Resources History*. Reston, VA: American Society of Civil Engineers, pp. 34–43. https://doi.org/10.1061/40650(2003)4.

Chevalier, C. and Bonelli, S. (2017) *Érosion interne dans les ouvrages hydrauliques. Volume 1: Méthodologie de caractérisation expérimentale*. Paris: Presses des Ponts.

ICOLD (2017) *L'érosion interne dans les digues, barrages existants et leurs fondations*. Bulletin 164. Paris: International Commission on Large Dams.

Lachouette, D. and Bonelli, S. (2008) 'Modélisation de l'érosion par renard hydraulique: du laboratoire à l'ouvrage', in *XXVIe Rencontres Universitaires de Génie Civil*. Nancy, France.

Temple, D.M. and Hanson, G.J. (1994) 'Headcut development in vegetated earth spillways', *Applied Engineering in Agriculture*, 10(5), pp. 677–682.

Wan, C.F. and Fell, R. (2004) 'Investigation of rate of erosion of soils in embankment dams', *Journal of Geotechnical and Geoenvironmental Engineering*, 130(4), pp. 373–380. https://doi.org/10.1061/(ASCE)1090-0241(2004)130:4(373).

How to cite this article:

Mady Sawadogo, Ulrich Landry Compaoré, Justin Tegawendé Zaïda and David Yemboini Kader Toguyeni. 2026. Reduced-Order Modelling of Concentrated-Leak Internal Erosion in the Former Zoungou Dam Embankment (Ganzourgou, Burkina Faso): Pipe Growth and Breach-Time Assessment. *Int.J.Curr.Res.Aca.Rev.* 14(11), 101-116. doi: https://doi.org/10.20546/ijcrar.2026.1411.012